arXiv:1209.5785v1 [cs.IT] 25 Sep 2012

Capacity Achieving Spatially Coupled Sparse Graph Modulation and Iterative Demodulation

Dmitri Truhachev and Christian Schlegel

September 27, 2012

Abstract

We consider a signalling format where information is modulated via a superposition of independent data streams. Each data stream is formed by simple replication and permutation of encoded information bits. Interconnection between data bits and modulation symbols transmitted over the channel can be represented in the form of a sparse graph. The modulated streams are transmitted by one or several users with a time offset enabling spatial coupling of the sparse modulation graphs. We prove that a two-stage demodulation/decoding method, in which iterative demodulation based on symbol estimation and interference cancellation is followed by parallel error correction decoding, achieves capacity of the additive white Gaussian noise (AWGN) channel.

1 Introduction

Recently, a technique of spatial graph coupling applied to iterative processing on graphs attracted significant interest in many areas of communications. The method was first introduced to construct low-density parity-check convolutional codes (LDPCCCs) [6] that exhibit a so called *threshold saturation* behaviour [12][13]. It has been proved that the asymptotic limit (threshold) of the suboptimal iterative decoding of LDPCCCs achieves the optimum maximum a posteriori probability (MAP) decoding threshold [13] in a variety of channels asymptotically. The idea of constructing graph structures from connected identical copies of a single graph has since been utilized to improve the performance of iterative methods in compressed sensing [7], image recognition, quantum coding [10], multi-user detection [8][9], and many other fields.

In this work we consider a communication format in which a sequence of modulated symbols at the transmitter is formed as a sum of equal power redundant independent data streams. The format is inspired by the multi-user modulation methods [4][5] permuting parts of the spread data sequences and has a few features common with multi-level coding [2], bit interleaved coded modulation [3], and repeat-accumulate codes [18]. A single data stream is formed by blocks of information bits that are first encoded for error correction, then replicated a number of times, and finally permuted. The main feature discussed in the paper is the data stream coupling accomplished by addition of the data streams (in real or complex domain) with a time offset. The receiver needs to carry out two tasks: suppression of the inter-stream interference and error correction decoding. We prove that these tasks can be efficiently accomplished by iterative data stream layering and subsequent error correction decoding performed for all data streams in parallel.

To find the data rate achieved by the proposed modulation format we study a system of equations describing the evolution of the noise-and-interference power experienced by each data stream throughout the detection iterations as a function of the iteration number and transmission time. We then prove that the achievable communication rate is within a small gap from the AWGN channel capacity and the gap disappears asymptotically as the signal-to-noise ratio (SNR) grows. This result is a counterpart of the result [11] showing that sparse graph modulation can achieve AWGN capacity with modified successive interference cancellation decoding. In this work we show that it is sufficient to perform demodulation and decoding sequentially. No feedback loop is required between the two processes.

The paper is organized as follows. The transmission format and the two-stage demodulation/decoding are described in Section 2. Section 3 presents a performance analysis and the proof of the main result. Numerical results are discussed in Section 4. Finally Section 5 concludes the paper.

2 System Model

We consider a modulation technique in which the signal transmitted over the channel is formed by a superposition of L independently modulated data streams. These streams may initiate at a single or multiple terminals and then superimpose at the receiver.

A schematic diagram of the modulator for one data stream is given in Figure 1. First a binary information sequence $\boldsymbol{u} = u_1, u_2, u_3, \cdots, u_K$ enters a binary forward error correction encoder of rate $R = K/N$. Then each bit of the encoded binary sequence $\boldsymbol{v} = v_1, v_2, v_3, \cdots, v_N$, where $v_j \in \{-1, 1\}$, is replicated M times. Finally the replicated data is permuted. In this paper we consider equal power data streams although generalization to unequal power streams is straightforward.

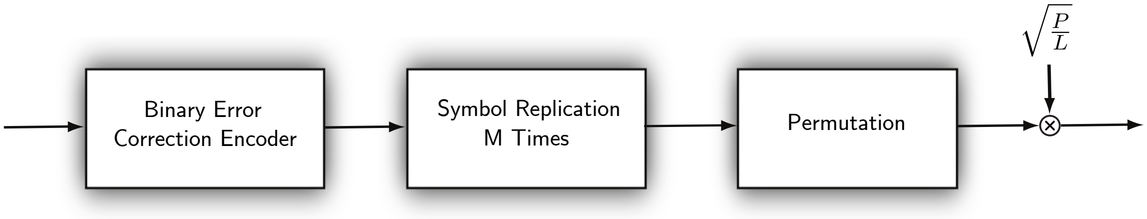

Figure 1: Modulation of one data stream.

The modulated signal $\boldsymbol{x} = (x_1, x_2, x_3, \cdots)$ is computed as the sum

$$x_t = \sum_{l=1}^{L} \tilde{v}_{t,l} \ , \tag{1}$$

where $\tilde{v}_{t,l}$ is the permuted and replicated data of the lth modulated data stream. The sequence $\boldsymbol{x}$ is multiplied by the power normalizing amplitude $\sqrt{P/L}$ and transmitted over the channel. In this paper we consider transmission over a real-valued AWGN channel. Thus, the received signal equals

$$\boldsymbol{y} = \sqrt{\frac{P}{L}}\boldsymbol{x} + \boldsymbol{n} \tag{2}$$

where $\boldsymbol{n} = (n_1, n_2, \cdots)$ is a noise vector with standard iid Gaussian components of zero mean and variance σ^2. The power of the modulated signal $x_t\sqrt{P/L}$ equals P since x_t is a sum (1) of L independent binary random variables attaining the values -1 and 1 with probability 1/2. Without loss of generality we can assume that $P = 1$. Therefore, the total signal-to-noise ratio (SNR) is normalized to $1/\sigma^2$. The total transmit data rate equals $RL/M = \alpha R$ information bits per channel use. The ratio $\alpha = L/M$ is called the *modulation load.*

2.1 Spatial Coupling of the Data Streams

In this paper we consider the case when L modulated data streams add up with an offset. Transmission of the first data stream starts at time $t = 1$. For the first $\tau_2 - 1$ symbol time intervals the modulated signal consists of a single data stream. After a delay of τ_2 symbols transmission of the second data stream is also initiated. For time instances $t \in [\tau_2, \tau_2 + \tau_3 - 1]$ the transmitted signal consists of a superposition (a sum) of two data streams. Then after a delay of τ_3 symbols the third data stream is also added and so on. Finally at time $t = m$ Lth data stream is added to the system. This process is illustrated in Figure 2 for the case of $L = 5$ streams and $\tau_2 = \tau_3 = \tau_4 = \tau_5 = 1$. In each data stream a transmitted block of MN data symbols is immediately followed by the next block. We call this process of transmission initialization *stream coupling.*

For the case of coupled data streams

$$x_t = \sum_{l=1}^{L(t)} \tilde{v}_{t,l} \qquad t \leq m \ . \tag{3}$$

where $L(t) \leq L$ denotes the number of data streams in the system at time t. We notice that the proposed modulation format allows for a graph representation in which variable nodes representing coded data bits v_j (before replication) are connected to channel nodes representing modulation symbols x_t. Therefore, the addition of data streams with an offset relates to spatial coupling of graphs representing modulated data streams.

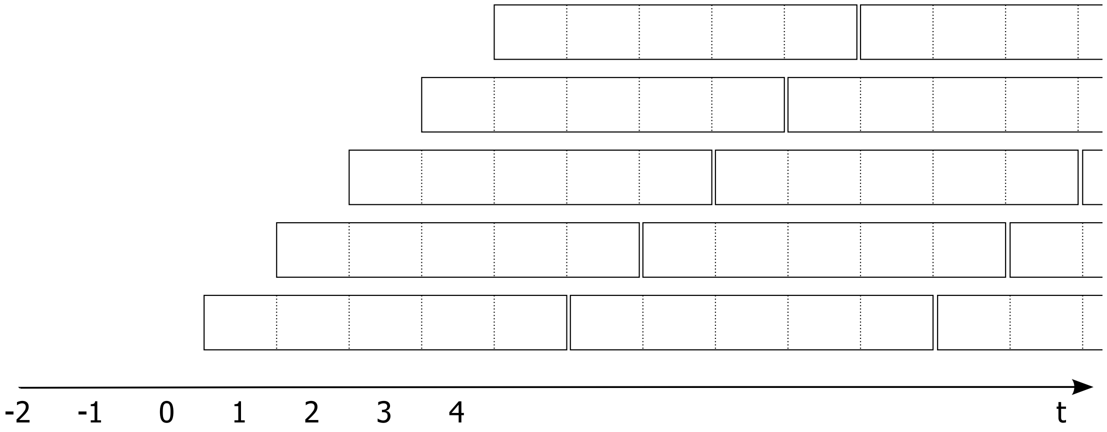

Figure 2: Coupled modulated data streams.

2.2 Iterative Demodulation and Decoding

The received signal $\boldsymbol{y}$ contains M replicas of each transmitted bit v_j, $j = 1, 2, \cdots$. Let $\mathcal{T}(j)$ denote the set of indices t such that the signal x_t, and therefore y_t, contains v_j. Moreover, by $\mathcal{J}(t)$ we denote a set of all indices j' such that $v_{j'}$ is included in y_t. For each bit v_j we use a set of received signals $\{y_t\}_{t\in\mathcal{T}(j)}$ to form a vector $\boldsymbol{y}_j$. Since each y_t, $t \in \mathcal{T}(j)$ contains v_j we have

$$\boldsymbol{y}_j = \boldsymbol{h} v_j + \boldsymbol{\xi}_j \tag{4}$$

where $\boldsymbol{h} = \sqrt{1/L}(1, 1, \cdots, 1)$. The vector $\boldsymbol{\xi}_j = (\xi_{j,t_1}, \xi_{j,t_2}, \cdots, \xi_{j,t_M})$, where $\mathcal{T}(j) = (t_1, t_2, \cdots, t_M)$ is the noise-and-interference vector with respect to the signal v_j. The components of the noise-and-interference vector are

$$\xi_{j,t} = \sqrt{\frac{1}{L}} \sum_{j'\in\mathcal{J}(t), j'\neq j} v_{j'} + n_t, \quad t \in \mathcal{T}(j) \ .$$

The vector ξ_j can be approximated a Gaussian random vector (due to central limit theorem) with independent zero-mean components and covariance matrix $\boldsymbol{R}_j = \mathrm{diag}(\sigma_{t_1}^2, \sigma_{t_2}^2, \cdots, \sigma_{t_M}^2)$ where σ_t^2 denotes the variance of $\xi_{j,t}$. For $t > m$ the cardinality of the set $\mathcal{J}(t)$ is $|\mathcal{J}(t)| = L$ giving the variance $\sigma_t^2 = (L-1)/L + 1$. However, since $|\mathcal{J}(t)| = L(t) < L$ for some $t \leq m$ and since the variances are influenced by the interference cancellation throughout the demodulation iterations we prefer to write a general expression based on σ_t^2.

We now perform minimum mean squared error (MMSE) filtering on $\boldsymbol{y}_j$ to form an estimate of v_j with the highest possible SNR. The output of this MMSE filter is

$$z_j = \boldsymbol{w}_j \boldsymbol{y}_j = \boldsymbol{w}_j \boldsymbol{h} v_j + \boldsymbol{w}_j \boldsymbol{\xi}_j \ , \tag{5}$$

where

$$\boldsymbol{w}_j = (\boldsymbol{I} + \boldsymbol{h}^* \boldsymbol{R}_j^{-1} \boldsymbol{h})^{-1} \boldsymbol{h}^* \boldsymbol{R}_j^{-1}$$

satisfies the minimization condition $||\boldsymbol{w}_j \boldsymbol{y}_j - v_j|| \to \min$. The resulting SNR of the signal z_j equals

$$\gamma_j = \boldsymbol{h}^* \boldsymbol{R}_j^{-1} \boldsymbol{h} = \frac{1}{L} \sum_{t\in\mathcal{T}(j)} \frac{1}{\sigma_t^2} \ . \tag{6}$$

Since $v_j \in \{1, -1\}$, and takes each of the two values with probability 1/2, we can form a conditional expectation estimate $\hat{v}_j$ of v_j as

$$\hat{v}_j = \mathbb{E}(v_j|z_j) = \tanh(z_j\gamma_j) = \tanh\left[z_j \frac{1}{L} \sum_{t\in\mathcal{T}(j)} \frac{1}{\sigma_t^2} \right] \ . \tag{7}$$

Once the estimates $\hat{v}_j$ are generated for all data bits v_j, $j = 1, 2, \cdots$ the next iteration starts with an interference cancellation step performed by computing

$$\boldsymbol{y}_j^{(1)} = \boldsymbol{h} v_j + \boldsymbol{\xi}_j^{(1)} \ , \tag{8}$$

where $\boldsymbol{h} = \sqrt{1/L}(1, 1, \cdots, 1)$ and

$$\xi_{j,t}^{(1)} = \sqrt{\frac{1}{L}} \sum_{j'\in\mathcal{J}(t), j'\neq j} (v_{j'} - \hat{v}_{j'}) + n_t \ . \tag{9}$$

We then proceed with calculating the new estimates $\hat{v}_j^{(1)}$ according to (5) and (7).

The estimation and interference cancellation process is repeated for a number of iterations. To avoid reusing the same information throughout the iterations we compute M vectors $\boldsymbol{y}_{j,t}^{(i)}$, $t \in \mathcal{T}(j)$ for each bit v_j at each iteration i. Vector $\boldsymbol{y}_{j,t}^{(i)}$ is composed of

$$y_{j,t'}^{(i)} = \sqrt{\frac{1}{L}} v_j + \sqrt{\frac{1}{L}} \sum_{j' \in \mathcal{J}(t'), j' \neq j} (v_{j'} - v_{j,t'}^{(i-1)}) + n_{t'} \tag{10}$$

where $t' \in \mathcal{T}(j), t' \neq t$. The vectors $\boldsymbol{y}_{j,t}^{(i)}$ are used to form M estimates $z_{j,t}^{(i)}$ according to (5) and corresponding $\hat{v}_{j,t}^{(i)}$ estimates according to (7).

We consider a two-stage decoding schedule. At the first stage I iterative demodulation iterations described above are performed. The second stage comprises simultaneous decoding of the forward error correction codes used to encode the information in the data streams prior to the modulation.

3 Performance Analysis

To simplify the derivation of the equations describing the evolution of the noise-and-interference power throughout the demodulation iterations we assume that each modulated data block of MN symbols consists of $2W+1$ equal length subblocks. Assume that the time t is measured in subblocks. We also assume that L data streams are split to $2W+1$ equal size groups with $L/(2W+1)$ data streams in each group. The transmission of the first group of streams starts at $t=1$, the transmission of the second group starts at $t=2$ and so on. This situation is illustrated in Figure 2 for the case of $W=2$.

The noise-and-interference power at iteration i and time t is given by

$$x_i^t \;=\; \frac{1}{2W+1} \sum_{j=-W}^{W} g_{\mathrm{m}} \left(\frac{1}{\alpha} \frac{1}{2W+1} \sum_{l=-W}^{W} \frac{1}{x_{i-1}^{t+j+l}} \right) + \sigma^2 \tag{11}$$

where the function $g_{\mathrm{m}}(\cdot)$, introduced in [19], is given by

$$g_{\mathrm{m}}(a) = \mathbb{E}\left[\left(1 - \tanh\left(a + \xi\sqrt{a}\right)\right)^2 \right] \;, \quad \xi \sim \mathcal{N}(0,1) \;,$$

and $\mathcal{N}(0,1)$ denotes a standard normal random variable. The recursion (11) was derived in [1] for a multi-user system in which data estimation and detection as well as interference cancellation are also described by (7) and (10). The total system power is normalized to 1 (i.e. individual data stream powers equal $1/\alpha$) and the noise power equals σ^2.

We assume that transmission starts at time $t=1$, i.e., the load of the system increases gradually. At every time instant t, the modulation load is increased by $\alpha/(2W+1)$ for $t = 1, 2, \cdots, 2W+1$. As a result, the initial condition for recursion (11) can be formulated as

$$x_0^t = 0 \quad t \leq 0 \;, \tag{12}$$

$$x_0^t = \frac{t}{2W+1} + \sigma^2; \quad t \in [1, 2W+1] \tag{13}$$

$$x_0^t = 1 + \sigma^2 \quad t > 2W+1 \;. \tag{14}$$

Following I demodulation iterations the residual noise-and-interference power of a data bit in a block transmitted at time t equals x_I^t. The error correction decoding performed at the second stage of the two-stage reception process is successful iff

$$\frac{1}{x_I^t} > \theta, \quad \forall t \tag{15}$$

where θ is the decoding threshold of the forward error correction code. The convergence of the SNR propagates along the received data stream with some speed s. Thus for each t the number of iterations required to achieve a specific SNR level needs to be $I(t) = st$, where s is a speed of convergence.

3.1 Roots of the Regular Convergence Equation

The convergence equation in the regular (uncoupled) case is

$$x_i = g_{\mathrm{m}}\left(\frac{1}{\alpha x_{i-1}}\right) + \sigma^2 \ . \tag{16}$$

In the uncoupled case when all the data streams are transmitted simultaneously with no time offset the system load equals α at any time t and all the data bits have the same SNR equal $\frac{1}{\alpha x_i}$ at iteration i irrespective of the time when the bits were transmitted. The corresponding equation

$$x = g_{\mathrm{m}}\left(\frac{1}{\alpha x}\right) + \sigma^2 \tag{17}$$

where $x \in [0, \infty)$ can have one, two, or three roots. We focus on the case when (17) has three roots $x^{(1)} < x^{(2)} < x^{(3)}$ and the uncoupled recursion (16) converges to the largest root $x^{(3)}$ while the coupled recursion (11) converges to the smallest root $x^{(1)}$ of (16). As we will see later (Lemma 1) $x^{(1)} \approx \sigma^2$ while $x^{(3)} \geq 0.3$ which means that at high SNR the coupled system may operate near channel capacity (Theorem 1) while the uncoupled system is deemed to have very low rate.

Note that the roots of (17) are functions of α and σ^2. For $\sigma^2 \geq 0.07$ we can define a threshold load value $\alpha_{\mathrm{s}}(\sigma^2)$ such that for $\alpha \in [0, \alpha_{\mathrm{s}}(\sigma^2))$ (17) has only one root, for $\alpha = \alpha_{\mathrm{s}}(\sigma^2)$ (17) has two roots, and for $\alpha \in (\alpha_{\mathrm{s}}(\sigma^2), \hat{\alpha}]$ (17) has three roots, where

$$\hat{\alpha} = \hat{\alpha}(\sigma^2) = 1/2 \log_2(1 + 1/\sigma^2) \ . \tag{18}$$

Figure 3 shows the function $g_{\mathrm{m}}\left(\frac{1}{\alpha x}\right) + \sigma^2$ plotted for $\sigma^2 = 0.01$ and three different values of α: $\alpha = 1.5$ (magenta curve), $\alpha = 2.0115 = \alpha_{\mathrm{s}}(0.01)$ (blue curve) and $\alpha = 2.5$ (green curve). The roots $x^{(1)}$, $x^{(2)}$, and $x^{(3)}$ are indicated for the case $\alpha = 2.5$. Lemma 1 states upper and lower bounds on the roots $x^{(1)}$ and $x^{(3)}$ which will be used in the proof of the main result.

Lemma 1. *(a) For $\sigma^2 \leq 1$ and $\alpha \in [0, \hat{\alpha}]$*

$$\sigma^2 \leq x^{(1)} \leq (1 + e^{-1/\sigma})\sigma^2 \leq 2\sigma^2 \ . \tag{19}$$

(b) For $\sigma^2 \leq 0.01$ and $\alpha \in [4, \hat{\alpha}]$

$$1 + \sigma^2 - \frac{2}{\alpha} \leq x^{(3)} \leq 1 + \sigma^2 \tag{20}$$

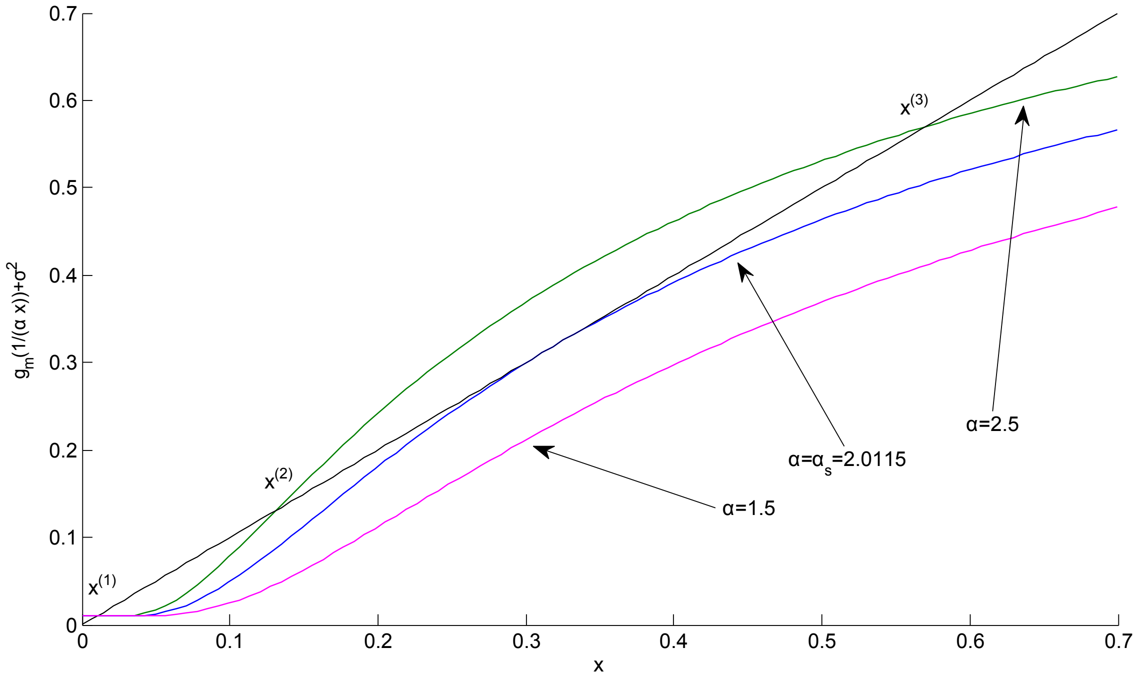

Figure 3: Plot of $g_{\mathrm{m}}(1/(x\alpha))+\sigma^2$ for $\sigma^2=0.01$ and $\alpha=1.5$ (magenta curve), $\alpha=2.0115=\alpha_{\mathrm{s}}(\sigma^2)$ (blue curve) and $\alpha=2.5$ (green curve).

(c) For $\sigma^2 \le 0.01$

$$x^{(3)} = 1+\sigma^2 - \frac{1}{\alpha(1+\sigma^2)} + o\left(\frac{1}{\alpha}\right) \tag{21}$$

(d) For $\sigma^2 \le 0.01$ *and* $\alpha \ge 2$

$$0.3 \le x^{(3)} \le 1+\sigma^2 \tag{22}$$

Proof. See Appendix A. □

Consider a recursion

$$x_i = g_{\mathrm{m}}\left(\frac{1}{\alpha(x_{i-1}+x^{(1)})}\right) + \sigma^2 - x^{(1)} \tag{23}$$

equivalent to (16) with respect to the shift of the roots by $x^{(1)} = x^{(1)}(\alpha,\sigma^2)$, the smallest root of (16). The roots of (23) equal $0, x^{(2)}-x^{(1)}, x^{(3)}-x^{(1)}$ where $x^{(1)}, x^{(2)}$, and $x^{(3)}$ are the roots of (16). Here by equivalence we mean that the two recursions always converge to the values which differ by $x^{(1)}(\alpha,\sigma^2)$. This can be easily shown by a variable exchange.

A coupled recursion corresponding to (23) can be constructed in a form similar to (11). The two coupled recursions are also equivalent from convergence perspective and the resulting sequences differ by $x^{(1)}(\alpha,\sigma^2)$.

3.2 Spectral Efficiency and Capacity

System (11) operates with total signal power 1 and noise power σ^2. The capacity of the (real-valued) AWGN channel for this parameters equals

$$\mathcal{C}_{\mathrm{AWGN}}(\sigma^2) = \frac{1}{2}\log_2\left(1 + \frac{1}{\sigma^2}\right) . \tag{24}$$

Assuming that the system (11) converges after limiting (infinite) number of iterations to the smallest root $x^{(1)}$ of (16) the achieved spectral efficiency is

$$\mathcal{C}_{\mathrm{eff}}(\alpha, \sigma^2) = \alpha \mathcal{C}_{\mathrm{BIAWGN}}\left(\frac{1}{\alpha x^{(1)}}\right) , \tag{25}$$

where $\mathcal{C}_{\mathrm{BIAWGN}}(\cdot)$ is the capacity of the binary-input AWGN (BIAWGN) channel as a function of the signal-to-noise ratio (SNR). Here we assume that the underlying forward error correction codes used for each data stream are optimal for the BIAWGN channel with SNR $\frac{1}{\alpha x^{(1)}}$ and therefore have rate $R = \mathcal{C}_{\mathrm{BIAWGN}}\left(\frac{1}{\alpha x^{(1)}}\right)$.

We are now ready to state the main result of the paper.

Theorem 1.

$$\mathcal{C}_{\mathit{eff}}(\alpha^*, \sigma^2) = \mathcal{C}_{\mathit{AWGN}}(\sigma^2) - \frac{\frac{3}{2\ln 2}}{\mathcal{C}_{\mathit{AWGN}}(\sigma^2)} + o\left(\frac{1}{\mathcal{C}_{\mathit{AWGN}}(\sigma^2)}\right) . \tag{26}$$

as $\sigma^2 \to 0$ *(and therefore* $\mathcal{C}_{\mathit{AWGN}}(\sigma^2) \to \infty$*). By* α^* *we denote the limiting modulation load value corresponding to* σ^2*.*

3.3 Proof of the Theorem 1

To prove the main theorem we derive a the convergence condition of the coupled system using a technique to study scalar recursions [17][15]. We then compute the achievable spectral efficiency (communication rate) and prove that it is within a small gap from the channel capacity.

We define two functions

$$f(x, \alpha) \overset{\mathrm{def}}{=} g_{\mathrm{m}}\left(\frac{1}{\alpha}\left(\frac{1}{x^{(1)}} - x\right)\right) + \sigma^2 - x^{(1)} , \tag{27}$$

$$g(x) \overset{\mathrm{def}}{=} \frac{1}{x^{(1)}} - \frac{1}{x^{(1)} + x} , \tag{28}$$

selected to ensure that the recursion

$$x_i = f(g(x_{i-1}), \alpha) = g_{\mathrm{m}}\left(\frac{1}{x_{i-1} + x^{(1)}}\right) + \sigma^2 - x^{(1)} \tag{29}$$

coincides with (23).

We consider $\sigma^2 \leq 1$ and for each value of σ^2 we consider $\alpha \in [0, \hat{\alpha}]$, where $\hat{\alpha}$ is defined in (18). The following lemma states the properties of the functions $f(x, \alpha)$ and $g(x)$.

Lemma 2. *For* $x \in [0, 1]$ *and* $\alpha \in [0, \hat{\alpha}]$

(a) $f(0,\alpha)=0$ *and* $f(x,0)=0$*,*

(b) $f(x,\alpha)$ *is an increasing function of* x*,*

(c) $g(0)=0$ *and* $g(x)$ *is an increasing function of* x*,*

(d) $f(g(x),\alpha)$ *is an increasing function of* α*.*

Proof. See Appendix B and Appendix C. □

We now compute the potential function of the system (29) in the form

$$U(x,\alpha) \overset{\text{def}}{=} \int_0^x (z - f(g(z),\alpha))\, g'(z) dz$$

$$= \ln \frac{x + x^{(1)}}{x^{(1)}} - \frac{\sigma^2 x}{x^{(1)}(x+x^{(1)})} - \alpha \int\limits_{\frac{1}{\alpha(x+x^{(1)})}}^{\frac{1}{\alpha x^{(1)}}} g_{\mathrm{m}}(y) dy \ . \tag{30}$$

Lemma 2 (c) and (d) imply that $U(x,\alpha)$ is a non-increasing function of α for any $x \in [0,1]$.

The method of potential functions [17] implies that a coupled version of system (23) converges to all-zero solution for $\alpha < \alpha^*$ satisfying

$$\alpha^* = \sup \left\{ \alpha : \min_{x\in[0,1]} U(x,\alpha) \geq 0 \right\} \ ,$$

when W is chosen to be sufficiently large. The function $U(x,\alpha)$ is plotted for $\sigma^2 = 0.0129$, 0.003347, and 0.000855 and the corresponding $\alpha^*(\sigma^2) = 3, 4, 5$ in Figure 4. Note that $\alpha^* = \alpha^*(\sigma^2)$ is a decreasing function of σ^2.

To find the minimum of $U(x,\alpha)$ for given α (and σ^2) we compute its partial derivative with respect to x

$$\frac{\partial U(x,\alpha)}{\partial x} = \frac{1}{x+x^{(1)}} - \frac{\sigma^2}{(x+x^{(1)})^2} - g_{\mathrm{m}}\left(\frac{1}{\alpha(x+x^{(1)})}\right) \frac{1}{(x+x^{(1)})^2} \ . \tag{31}$$

The condition for extremum

$$\frac{\partial U(x,\alpha)}{\partial x} = 0 \tag{32}$$

is equivalent to

$$x + x^{(1)} = g_{\mathrm{m}}\left(\frac{1}{\alpha(x+x^{(1)})}\right) + \sigma^2 \ . \tag{33}$$

Depending on the value of α we can consider there cases (see Section 3.1)

1. *In case* $\alpha \in [0, \alpha_s)$ equation (33) has a single root $x = 0$ corresponding to the minimum of $U(x,\alpha)$. This implies $U(x,\alpha) \geq 0$ for $x \in [0,1]$.

2. *In case* $\alpha = \alpha_s$ equation (33) has two roots: $x = 0$ corresponding to the minimum and $x = x^{(2)} - x^{(1)}$ corresponding to a maximum of $U(x,\alpha)$. Again this implies $U(x,\alpha) \geq 0$ for $x \in [0,1]$.

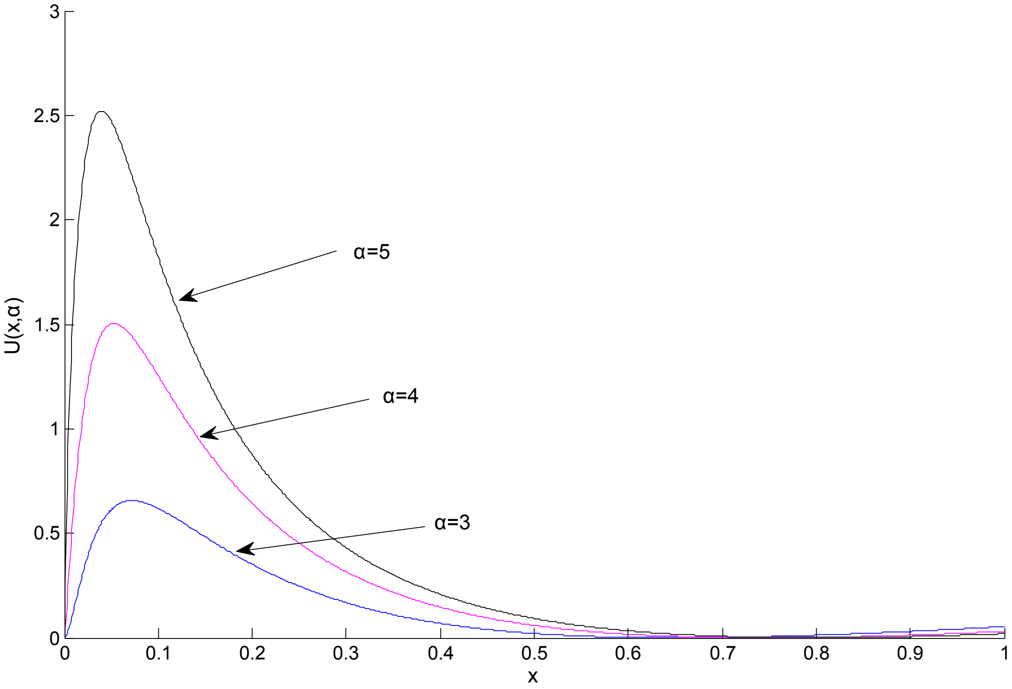

Figure 4: Plot of $U(x,\alpha)$ for $\alpha = 3$ and $\sigma^2 = 0.0129$ (blue curve), $\alpha = 4$ and $\sigma^2 = 0.003347$ (magenta curve), and $\alpha = 5$ and $\sigma^2 = 0.000855$ (black curve).

3. *Case* $\alpha \in (\alpha_s, \hat{\alpha})$ corresponds to the case when (33) has three roots. $U(x,\alpha)$ has two local minimums and the second minimum, located at the point $x_{\mathrm{m}} = x^{(3)} - x^{(1)}$, can be negative for large α (the first local minimum is at $x = 0$).

Therefore the value of x for which $U(x, \alpha^*) = 0$ equals $x_{\mathrm{m}} = x^{(3)} - x^{(1)}$ and corresponds to Case 3. Computing $U(x_{\mathrm{m}}, \alpha)$ gives

$$U(x_{\mathrm{m}}, \alpha) = U(x^{(3)} - x^{(1)}, \alpha) = \ln \frac{x^{(3)}}{x^{(1)}} - \frac{x^{(3)} - x^{(1)}}{x^{(1)} x^{(3)}} \sigma^2 - \alpha \int\limits_{\frac{1}{\alpha x^{(3)}}}^{\frac{1}{\alpha x^{(1)}}} g_{\mathrm{m}}(y) dy \ . \tag{34}$$

To find α^* we consider equality

$$U(x^{(3)} - x^{(1)}, \alpha) = 0 \tag{35}$$

which is equivalent to

$$\ln \frac{x^{(3)}}{x^{(1)}} - \frac{x^{(3)} - x^{(1)}}{x^{(1)} x^{(3)}} \sigma^2 - \alpha \int\limits_{\frac{1}{\alpha x^{(3)}}}^{\frac{1}{\alpha x^{(1)}}} g_{\mathrm{m}}(y) dy = 0 \tag{36}$$

$$\ln \frac{x^{(3)}}{x^{(1)}} - \frac{x^{(3)} - x^{(1)}}{x^{(1)} x^{(3)}} \sigma^2 - \alpha 2 \ln 2 \left(\mathcal{C}_{\mathrm{BIAWGN}} \left(\frac{1}{\alpha x^{(1)}} \right) - \mathcal{C}_{\mathrm{BIAWGN}} \left(\frac{1}{\alpha x^{(3)}} \right) \right) = 0 \tag{37}$$

where the last equality of the left hand side is due a relationship between MMSE (i.e. function $g_{\mathrm{m}}(\cdot)$) and the mutual information for BIAWGN channel, derived in [14]. Continuing with dividing (37) by $2\ln 2$ we define a function

$$\begin{aligned} u(\alpha) \overset{\mathrm{def}}{=} & \frac{1}{2}\log_2 \frac{x^{(3)}(\alpha,\sigma^2)}{x^{(1)}(\alpha,\sigma^2)} - \frac{1}{2\ln 2}\frac{x^{(3)}(\alpha,\sigma^2)-x^{(1)}(\alpha,\sigma^2)}{x^{(1)}(\alpha,\sigma^2)x^{(3)}(\alpha,\sigma^2)}\sigma^2 \\ & - \alpha\left(\mathcal{C}_{\mathrm{BIAWGN}}\left(\frac{1}{\alpha x^{(1)}(\alpha,\sigma^2)}\right) - \mathcal{C}_{\mathrm{BIAWGN}}\left(\frac{1}{\alpha x^{(3)}(\alpha,\sigma^2)}\right)\right) \end{aligned} \tag{38}$$

where for fixed σ^2

$$u(\alpha) > 0 \quad \text{for} \quad \alpha \in (\alpha_{\mathrm{s}}, \alpha^*) \tag{39}$$

$$u(\alpha^*) = 0 \ . \tag{40}$$

Now we estimate α^* using (38), (39), and (40). Applying the bounds on $x^{(1)}$ and $x^{(3)}$ given in Lemma 1 to some parts of the expression (38) we obtain

$$\begin{aligned} u(\alpha) \geq & \frac{1}{2}\log_2 \frac{x^{(3)}}{(1+e^{-1/\sigma})\sigma^2} - \frac{\sigma^2}{2\ln 2}\frac{1+\sigma^2-\sigma^2}{\sigma^2 x^{(3)}} \\ & - \alpha\left(\mathcal{C}_{\mathrm{BIAWGN}}\left(\frac{1}{\alpha(1+e^{-1/\sigma})\sigma^2}\right) - \mathcal{C}_{\mathrm{BIAWGN}}\left(\frac{1}{\alpha(1+\sigma^2)}\right)\right) \ . \end{aligned} \tag{41}$$

The next step is an application of the bounds on the capacity of BIAWGN channel

$$\frac{\gamma-\gamma^2}{2\ln 2} \leq \mathcal{C}_{\mathrm{BIAWGN}}(\gamma) \leq 1 \ . \tag{42}$$

The lower bound in (42) derived in [20][16] is valid for $\gamma < 1$ and we apply it to the last term in (41)

$$\mathcal{C}_{\mathrm{BIAWGN}}\left(\frac{1}{\alpha(1+\sigma^2)}\right) \geq \frac{1}{2\ln 2\alpha(1+\sigma^2)} - \frac{1}{2\ln 2\alpha^2(1+\sigma^2)^2} \tag{43}$$

since $\alpha(1+\sigma^2) > 1$ for $\alpha \geq \alpha_{\mathrm{s}} > 1$. The upper bound of (42) is used to derive

$$\mathcal{C}_{\mathrm{BIAWGN}}\left(\frac{1}{\alpha(1+e^{-1/\sigma})\sigma^2}\right) \leq 1 \tag{44}$$

Using the BIAWGN channel capacity bounds (43) and (44) in (41) we obtain

$$u(\alpha) \geq \frac{1}{2}\log_2 \frac{x^{(3)}}{(1+e^{-1/\sigma})\sigma^2} - \frac{1}{2\ln 2}\frac{1}{x^{(3)}} - \alpha + \frac{1}{2\ln 2(1+\sigma^2)} - \frac{1}{2\ln 2\alpha(1+\sigma^2)^2} \tag{45}$$

$$\begin{aligned} = & \frac{1}{2}\log_2 \frac{1+\sigma^2}{\sigma^2} - \alpha + \frac{1}{2}\log_2 \frac{x^{(3)}}{(1+\sigma^2)(1+e^{-1/\sigma})} - \frac{1}{2\ln 2}\frac{1}{x^{(3)}} \\ & + \frac{1}{2\ln 2(1+\sigma^2)} - \frac{1}{2\ln 2\alpha(1+\sigma^2)^2} \end{aligned} \tag{46}$$

$$= \frac{1}{2}\log_2 \frac{1+\sigma^2}{\sigma^2} - \alpha + \xi(\alpha) = \hat{\alpha} - \alpha + \xi(\alpha) \tag{47}$$

where

$$\xi(\alpha) \overset{\mathrm{def}}{=} \frac{1}{2}\log_2 \frac{x^{(3)}}{(1+e^{-1/\sigma})(1+\sigma^2)} - \frac{1}{2\ln 2}\frac{1}{x^{(3)}} + \frac{1}{2\ln 2(1+\sigma^2)} - \frac{1}{2\ln 2\alpha(1+\sigma^2)^2} \ . \tag{48}$$

Applying the asymptotic expression (c) of Lemma 1 we obtain an asymptotic expression for $\xi(\alpha)$

$$\begin{aligned}\xi(\alpha) = \frac{1}{2\ln 2}\Bigg[&\ln \frac{1+\sigma^2-\frac{1}{\alpha(1+\sigma^2)}+o\left(\frac{1}{\alpha}\right)}{(1+e^{-1/\sigma})(1+\sigma^2)} \\ &-\frac{1}{1+\sigma^2-\frac{1}{\alpha(1+\sigma^2)}+o\left(\frac{1}{\alpha}\right)}+\frac{1}{1+\sigma^2}-\frac{1}{\alpha(1+\sigma^2)^2}\Bigg]\end{aligned} \tag{49}$$

$$\begin{aligned}= -\frac{\ln(1+e^{-1/\sigma})}{2\ln 2}+\frac{1}{2\ln 2}\Bigg[&\ln\left(1-\frac{1}{\alpha(1+\sigma^2)^2}+o\left(\frac{1}{\alpha}\right)\right) \\ &+\frac{-\frac{1}{\alpha(1+\sigma^2)}+o\left(\frac{1}{\alpha}\right)}{\left(1+\sigma^2-\frac{1}{\alpha(1+\sigma^2)}+o\left(\frac{1}{\alpha}\right)\right)(1+\sigma^2)}-\frac{1}{\alpha(1+\sigma^2)^2}\Bigg]\end{aligned} \tag{50}$$

$$= -\frac{\ln(1+e^{-1/\sigma})}{2\ln 2}+\frac{1}{2\ln 2}\left[-\frac{1}{\alpha(1+\sigma^2)^2}+o\left(\frac{1}{\alpha}\right)-\frac{1}{\alpha(1+\sigma^2)^3}-\frac{1}{\alpha(1+\sigma^2)^2}\right] \tag{51}$$

$$= -\frac{\ln(1+e^{-1/\sigma})}{2\ln 2}+\frac{1}{2\ln 2}\left[-\frac{2}{\alpha(1+\sigma^2)^2}-\frac{1}{\alpha(1+\sigma^2)^3}+o\left(\frac{1}{\alpha}\right)\right] \ . \tag{52}$$

Finally a combination of (47) and (52) implies

$$u(\alpha) \geq \hat{\alpha}-\alpha+\xi(\alpha) = \hat{\alpha}-\alpha+B+\frac{C}{\alpha}+o\left(\frac{1}{\alpha}\right) \ , \tag{53}$$

where

$$B = -\frac{\ln(1+e^{-1/\sigma})}{2\ln 2} \ , \tag{54}$$

$$C = -\frac{1}{2\ln 2}\left[\frac{2}{(1+\sigma^2)^2}+\frac{1}{(1+\sigma^2)^3}\right] \ . \tag{55}$$

Now we consider equation

$$\hat{\alpha}-\alpha+B+\frac{C}{\alpha}=0$$

and its largest root

$$\alpha_{\mathrm{r}} = \frac{\hat{\alpha}+B}{2}\left(1+\sqrt{1+\frac{4C}{(\hat{\alpha}+B)^2}}\right) = \hat{\alpha}+B+\frac{C}{(\hat{\alpha}+B)^2}+o\left(\frac{1}{\hat{\alpha}}\right) \tag{56}$$

Since α^* is the root of $u(\alpha)$ and $u(\alpha) > 0$ for $\alpha < \alpha^*$ from (53) we obtain

$$\alpha^* = \alpha_{\mathrm{r}} + o\left(\frac{1}{\hat{\alpha}}\right) \ .$$

Using the fact that $\mathcal{C}_{\mathrm{AWGN}}(\sigma^2) = \hat{\alpha}$ (see Section 3.2) and taking into account

$$B = o\left(\frac{1}{\hat{\alpha}}\right) \tag{57}$$

$$C = \frac{3}{2\ln 2}+o\left(\frac{1}{\hat{\alpha}}\right) \tag{58}$$

we find that

$$\alpha^* = \mathcal{C}_{\text{AWGN}}(\sigma^2) - \frac{\frac{3}{2\ln 2}}{\mathcal{C}_{\text{AWGN}}(\sigma^2)} + o\left(\frac{1}{\mathcal{C}_{\text{AWGN}}(\sigma^2)}\right) . \tag{59}$$

as $\sigma^2 \to 0$ and $\mathcal{C}_{\text{AWGN}}(\sigma^2) \to \infty$. The achievable spectral efficiency (see Section 3.2) equals

$$\mathcal{C}_{\text{eff}}(\alpha^*, \sigma^2) = \alpha^* \mathcal{C}_{\text{BIAWGN}}\left(\frac{1}{\alpha^* x^{(1)}}\right) . \tag{60}$$

From (38) and (40) we obtain

$$\begin{aligned}\mathcal{C}_{\text{eff}}(\alpha^*, \sigma^2) &= \frac{1}{2}\log_2 \frac{x^{(3)}(\alpha^*, \sigma^2)}{x^{(1)}(\alpha^*, \sigma^2)} \\ &\quad - \frac{1}{2\ln 2}\frac{x^{(3)}(\alpha^*, \sigma^2) - x^{(1)}(\alpha^*, \sigma^2)}{x^{(1)}(\alpha^*, \sigma^2)x^{(3)}(\alpha^*, \sigma^2)}\sigma^2 - \alpha^* \mathcal{C}_{\text{BIAWGN}}\left(\frac{1}{\alpha x^{(3)}(\alpha^*, \sigma^2)}\right) \qquad (61) \\ &= \hat{\alpha} + \xi(\alpha^*) \qquad (62)\end{aligned}$$

where the last equality comes from (45)–(47). Combing the above with (52) and (59) finally gives the main result

$$\mathcal{C}_{\text{eff}}(\alpha^*, \sigma^2) = \mathcal{C}_{\text{AWGN}}(\sigma^2) - \frac{\frac{3}{2\ln 2}}{\mathcal{C}_{\text{AWGN}}(\sigma^2)} + o\left(\frac{1}{\mathcal{C}_{\text{AWGN}}(\sigma^2)}\right) .$$

Theorem 1 is proved.

4 Numerical Results and Discussion

The asymptotic expression in Theorem 1 demonstrates the asymptotic behaviour of the spectral efficiency and shows that the gap between the spectral efficiency and the AWGN channel capacity tends to zero as SNR increases. For small SNR we can obtain limiting system loads α^* numerically. The gap between the achievable spectral efficiency and the AWGN channel capacity is plotted in Figure 5. We can observe that the gap is decreasing as the SNR and the channel capacity grows.

5 Conclusion

We consider modulation of information in a form a superposition of independent equal power and rate data streams. Each streams is formed by repetition and permutation of data and the streams are added up with an offset initiating the effect of "stream coupling". We prove that the proposed system used with iterative demodulation followed by error correction deciding at the receiver achieves capacity of the AWGN channel asymptotically.

References

[1] C. Schlegel and D. Truhachev,"Multiple Access Demodulation in the Lifted Signal Graph with Spatial Coupling," *IEEE Transactions on Information Theory*, under revision, March 2011.

[2] H. Imai and S. Hirakawa, "A new multilevel coding method using error correcting codes," *IEEE Transactions on Information Theory*, vol. 23, pp. 371–377, May 1977.

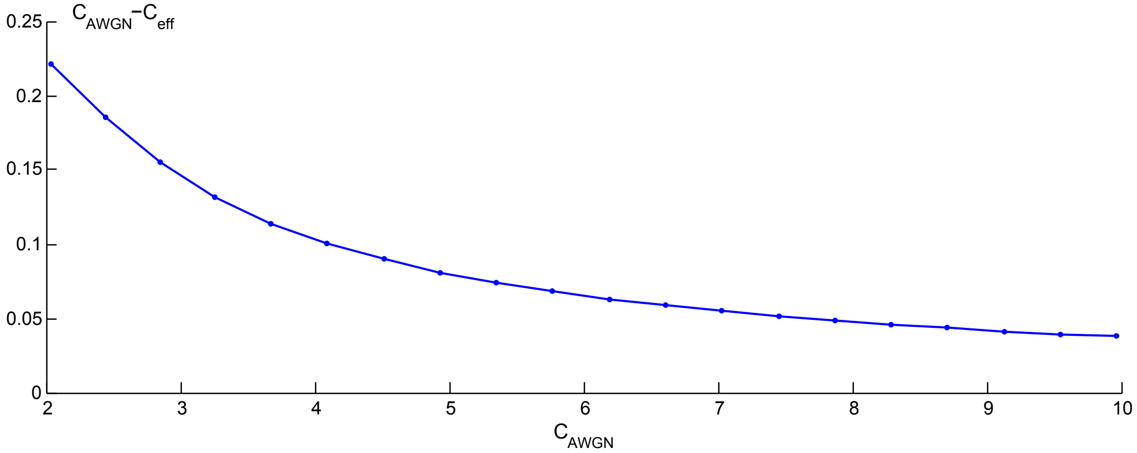

Figure 5: Gap between achieved spectral efficiency and the channel capacity (in bits) plotted as a function of channel capacity.

[3] G. Caire, G. Taricco, and E. Biglieri, “Bit-interleaved coded modulation,” *IEEE Trans. Inform. Theory*, vol. 44, pp. 927–946, May 1998.

[4] C. Schlegel, M. Burnashev, and D. Truhachev, “Generalized superposition modulation and iterative demodulation: A capacity investigation,” *Hindawi Journal of Electr. and Comp. Eng.*, vol. 2010, Sep. 2010.

[5] D. Truhachev, C. Schlegel, and L. Krzymien, “A two-stage capacity-achieving demodulation/decoding method for random matrix channels,” *IEEE Tran. on Inform. Theory*, vol. 55, no. 1, pp. 136–146, Jan. 2009.

[6] A. Jiménez Felström and K. Sh. Zigangirov, “Time-varying periodic convolutional codes with low-density parity-check matrices,” *IEEE Trans. Inf. Theory*, vol. 45, no. 6, pp. 2181–2191, Sept. 1999.

[7] S. Kudekar and H. D. Pfister, “The effect of spatial coupling on compressive sensing,” in *Proc. Allerton Conf. on Communications, Control, and Computing*, Monticello, IL, Sept. 2010.

[8] C. Schlegel and D. Truhachev, “Multiple Access Demodulation in the Lifted Signal Graph with Spatial Coupling,” in *Proc. IEEE Int. Symp. on Inf. Theory*, St. Petersburg, Russia, Aug. 2011.

[9] K. Takeuchi, T. Tanaka, and T. Kawabata, “Improvement of BP-based CDMA multiuser detection by spatial coupling,” in *Proc. IEEE Int. Symp. on Inf. Theory*, St. Petersburg, Russia, Aug. 2011.

[10] M. Hagiwara, K. Kasai, H. Imai, and K. Sakaniwa, “Spatially coupled quasi-cyclic quantum LDPC codes,” in *Proc. IEEE Int. Symp. on Inf. Theory*, St. Petersburg, Russia, Aug. 2011.

[11] D. Truhachev, “Achieving AWGN Multiple Access Channel Capacity with Spatial Graph Coupling,” *IEEE Communications Letters*, vol. 16, no. 5, pp. 585–588, May 2012.

[12] M. Lentmaier, A. Sridharan, D. J. Costello, Jr., and K. Sh. Zigangirov, “Iterative decoding threshold analysis for LDPC convolutional codes,” *IEEE Trans. Inf. Theory*, vol. 56, no. 10, pp. 5274–5289, Oct. 2010.

[13] S. Kudekar, T. J. Richardson, and R. L. Urbanke, “Threshold saturation via spatial coupling: why convolutional LDPC ensembles perform so well over the BEC,” *IEEE Trans. Inf. Theory*, vol. 57, no. 2, pp. 803–834, Feb. 2011.

[14] D. Guo, S. Shamai, and S. Verdu, “Mutual Information and Minimum Mean-Square Error in Gaussian Channels,” *IEEE Trans. Inf. Theory*, vol. 51, no. 4, pp. 1261–1282, April 2005.

[15] S. Kudekar, T. J. Richardson, and R. L. Urbanke, “Wave-Like Solutions of General One-Dimensional Spatially Coupled Systems,” submitted to *IEEE Trans. Inf. Theory*, 2012, arXiv:1208.3273.

[16] M. S. Alencar, “A comparison of bounds on the capacity of a binary channel,” in *Proc. Global Telecommun. Conf.*, Nov. 1996, vol. 2, pp. 1273–1275.

[17] A. Yedla, Y.-Y. Jian, P. S Nguyen and H. D. Pfister, “A Simple Proof of Threshold Saturation for Coupled Scalar Recursions,” in *7th International Symposium on Turbo Codes and Iterative Information Processing*, Gothenburg, Sweden, August 2012.

[18] D. Divsalar, H. Jin, and R. J. McEliece, “Coding theorems for turbo-like codes,” *in Proc. 36th Allerton Conf. on Communication, Control, and Computing*, pp. 201–210, Allerton, Illinois, USA, Sept. 1998.

[19] M. Burnashev, C. Schlegel, W. Krzymien, and Z. Shi, “Characteristics Analysis of Successive Interference Cancellation Methods”, *Problemy Peredachi Informatsii*, vol. 40, no. 4, pp. 297–317, Dec. 2004.

[20] R. Gallager, *Information Theory and Reliable Communications*, Wiley & Sons, New York, 1968.

A Proof of Lemma 1

We start with deriving the bound on $x^{(1)}$. The lower bound is trivial since $g_{\mathrm{m}}(y) > 0$, for $y \in (0, \infty)$ implies

$$\sigma^2 \leq x^{(1)} = g_{\mathrm{m}}\left(\frac{1}{\alpha x^{(1)}}\right) + \sigma^2 \ . \tag{63}$$

To derive an upper bound on $x^{(1)}$ we notice that

$$\sigma^2 < g_{\mathrm{m}}\left(\frac{1}{\alpha \sigma^2}\right) + \sigma^2 \ . \tag{64}$$

which again follows from the fact that $g_{\mathrm{m}}(\cdot)$ in non-negative and show that

$$2\sigma^2 > g_{\mathrm{m}}\left(\frac{1}{\alpha \cdot 2\sigma^2}\right) + \sigma^2 \ . \tag{65}$$

To prove (65) we start with

$$g_{\mathrm{m}}\left(\frac{1}{\alpha 2\sigma^2}\right) + \sigma^2 \leq \pi Q\left(\frac{1}{\sqrt{\alpha 2\sigma^2}}\right) + \sigma^2 \tag{66}$$

which follows from an upper bound on $g_{\mathrm{m}}(\cdot)$ derived in [19]. Continuing upper bounding $Q(\cdot)$ and using $\alpha \leq \hat{\alpha}$ we obtain

$$\begin{aligned} x^{(1)} &\le \pi Q\left(\frac{1}{\sqrt{\hat{\alpha}2\sigma^2}}\right) + \sigma^2 \le \pi \frac{1}{\sqrt{2\pi}}\sqrt{\hat{\alpha}2\sigma^2}\exp\left(-\frac{1}{\hat{\alpha}\sigma^2}\right) + \sigma^2 && (67)\\ &= \exp\left(-\frac{1}{\hat{\alpha}\sigma^2} + \frac{1}{2}\ln\frac{\pi}{2} + \frac{1}{2}\ln(2\sigma^2\hat{\alpha})\right) + \sigma^2 && (68)\\ &= \exp\left(-\frac{1}{\sigma^2\frac{1}{2\ln 2}\ln(1+1/\sigma^2)} + \frac{1}{2}\ln\frac{\pi}{2} + \frac{1}{2}\ln\left(2\sigma^2\frac{1}{2\ln 2}\ln(1+1/\sigma^2)\right)\right) + \sigma^2 && (69)\\ &\le \exp\left(-\frac{1}{\sigma} + 2\ln(\sigma)\right) + \sigma^2 < 2\sigma^2 \ . && (70) \end{aligned}$$

The first inequality in (70) is valud for $\sigma^2 \le 1$ and is due to the fact that the term $-1/\sigma^2$ dominates the exponent in (69) as $\sigma^2 \to 0$. The bound (65) is proved.

Bounds (64) and (65) imply existence of the root $\sigma^2 \le x^{(1)} \le 2\sigma^2$ for any $\alpha \in [0, \hat{\alpha}]$ when $\sigma^2 \le 1$. The root $x^{(1)}$ then satisfies (70). Lemma 1 (a) is proved.

The upper bound on $x^{(3)}$ is again trivial since $g_{\mathrm{m}}(y) \le 1$ for $y \in [0, \infty]$ and therefore

$$x^{(3)} = g_{\mathrm{m}}\left(\frac{1}{\alpha x^{(3)}}\right) + \sigma^2 \le 1 + \sigma^2 \ .$$

To prove the lower bound we use the bound

$$g_{\mathrm{m}}(y) \ge 1 - y \qquad (71)$$

valid for $y \in [0, \infty]$, derived in [19]. Inequality (71) implies that the largest root of the equation

$$x = 1 - \frac{1}{\alpha x} + \sigma^2$$

is a lower bound on $x^{(3)}$. Therefore

$$\begin{aligned} x^{(3)} &\ge \frac{1+\sigma^2}{2}\left(1 + \sqrt{1 - \frac{4}{\alpha(1+\sigma^2)^2}}\right) && (72)\\ &\ge \frac{1+\sigma^2}{2}\left(1 + 1 - \frac{4}{\alpha(1+\sigma^2)^2}\right) \ge 1 + \sigma^2 - \frac{2}{\alpha} \ . && (73) \end{aligned}$$

Since the value inside the square root in (72) needs to be non-negative the bound can be used for

$$\frac{4}{(1+\sigma^2)^2} \le \alpha \ ,$$

i.e., essentially for $\alpha \ge 4$. Lemma 1 (b) is proved.

Applying asymptotic expression

$$g_{\mathrm{m}}(y) = 1 - y + o(y) \quad \text{for } y \to 0$$

obtained in [19] we find that for $\alpha \to \infty$ and $x \le 1 + \sigma^2$

$$g_{\mathrm{m}}\left(\frac{1}{\alpha x}\right) + \sigma^2 = 1 - \frac{1}{\alpha x} + \sigma^2 + o\left(\frac{1}{\alpha}\right) \ .$$

This implies that (72) gives an asymptotic expression

$$x^{(3)} = 1 + \sigma^2 - \frac{1}{\alpha(1+\sigma^2)} + o\left(\frac{1}{\alpha}\right) \ . \tag{74}$$

Lemma 1 (c) is proved.

To derive a bound useful for $\alpha < 4$ we start with showing that $\alpha_\mathrm{s}(\sigma^2)$ is a decreasing function of σ^2. We observe that $\alpha_\mathrm{s}(\sigma^2)$ can alternatively be defined as a value of α satisfying

$$\max_{x \geq x^{(1)}} \frac{1}{x} g_\mathrm{m}\left(\frac{1}{\alpha x}\right) + \frac{1}{x}\sigma^2 = 1 \ , \tag{75}$$

where the maximum is achieved at $x^{(2)}(\alpha_\mathrm{s}(\sigma^2), \sigma^2) = x^{(3)}(\alpha_\mathrm{s}(\sigma^2), \sigma^2)$. Clearly, for any $\tilde{\sigma}^2 < \sigma^2$

$$\frac{1}{x^{(3)}(\alpha_\mathrm{s}(\sigma^2), \sigma^2)} g_\mathrm{m}\left(\frac{1}{\alpha x^{(3)}(\alpha_\mathrm{s}(\sigma^2), \sigma^2)}\right) + \frac{\tilde{\sigma}^2}{x^{(3)}(\alpha_\mathrm{s}(\sigma^2), \sigma^2)} < 1$$

and therefore $\alpha_\mathrm{s}(\tilde{\sigma}^2) > \alpha_\mathrm{s}(\sigma^2)$ and the corresponding $x^{(3)}(\tilde{\sigma}^2)$ will bring the maximum to 1. Since $\alpha_\mathrm{s}(\sigma^2)$ is a decreasing function of σ^2 then for any $\sigma^2 > 0$

$$\alpha_\mathrm{s}(\sigma^2) < \alpha_\mathrm{s}(0) \approx 2.0756 \ . \tag{76}$$

Our second step is to show that $\alpha_\mathrm{s}(\sigma^2)x^{(3)}$ where $x^{(3)}$ is the root corresponding to $\alpha_\mathrm{s}(\sigma^2)$ is also a decreasing function of σ^2. By a variable exchange $y = 1/(\alpha x)$ in equality (75) we transform it to an equivalent form

$$\frac{1}{\alpha}\left(y_\mathrm{r} g_\mathrm{m}(y_\mathrm{r}) + y_\mathrm{r}\sigma^2\right) = 1 \tag{77}$$

where y_r is a root of

$$\frac{d}{dy}\frac{1}{\alpha}\left(y g_\mathrm{m}(y) + y\sigma^2\right) = \frac{1}{\alpha}\left(y g_\mathrm{m}'(y) + g_\mathrm{m}(y) + \sigma^2\right) = 0 \tag{78}$$

corresponding to the local maximum of $s(y) = y g_\mathrm{m}(y) + y\sigma^2$. Function $s(y)$ has a single extremum maximum for $\sigma^2 \leq 0.01$. Function $h(y) = y g_\mathrm{m}(y)$ (blue curve) and its derivative (magenta curve) are plotted in Figure 6. It is easy to notice that the value y_r corresponding to the maximum of $s(y)$ is an increasing function of σ^2 and therefore $\alpha_\mathrm{s}(\sigma^2)x^{(3)} = 1/y_\mathrm{r}$ decreases with σ^2. Thus for arbitrary $\sigma^2 \leq 0.01$

$$\alpha_\mathrm{s}(\sigma^2)x^{(3)}(\sigma^2) > \alpha_\mathrm{s}(0.01)x^{(3)}(0.01) \tag{79}$$

which leads to

$$x^{(3)}(\sigma^2) > \frac{1}{\alpha_\mathrm{s}(\sigma^2)}\alpha_\mathrm{s}(0.01)x^{(3)}(0.01) > \frac{\alpha_\mathrm{s}(0.01)}{\alpha_\mathrm{s}(0)}x^{(3)}(0.01) = \frac{2.0115}{2.0756}0.3180 = 0.3082 \ , \tag{80}$$

with an application of (76). Lemma 1 (d) is proved.

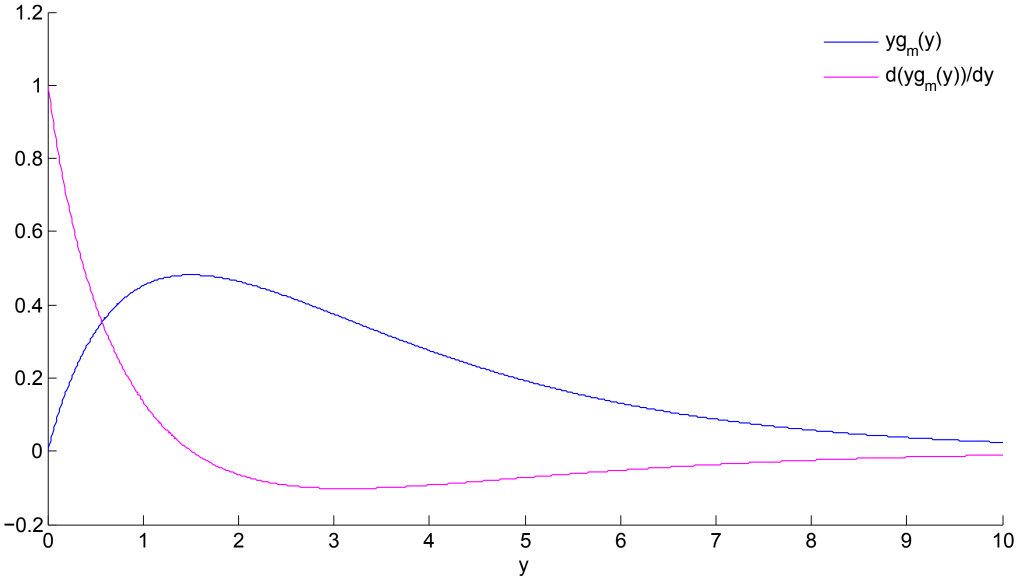

Figure 6: Plot of $yg_{\mathrm{m}}(y)$ (blue curve) and its derivative (magenta curve).

B Proof of Lemma 2, (a)–(c)

We start with proving property (a). The first statement

$$f(0,\alpha) = g_{\mathrm{m}}\left(\frac{1}{\alpha x^{(1)}}\right) + \sigma^2 - x^{(1)} = 0 \tag{81}$$

follows from the definition of $x^{(1)}$ which is a root of (16). To prove the second statement we note that for $\alpha = 0$ equation (16) transforms into

$$x = \sigma^2 \ . \tag{82}$$

As a result $x^{(1)} = \sigma^2$ and therefore for $\alpha = 0$

$$f(x,0) = \lim_{\alpha\to 0} g_{\mathrm{m}}\left(\frac{1}{\alpha}\left(\frac{1}{x^{(1)}} - x\right)\right) + \sigma^2 - x^{(1)} = \sigma^2 - x^{(1)} = 0 \ . \tag{83}$$

Property (b) can be easily verified since $g_{\mathrm{m}}(\cdot)$ is a strictly decreasing [19] function and therefore

$$f(x,\alpha) = g_{\mathrm{m}}\left(\frac{1}{\alpha}\left(\frac{1}{x^{(1)}} - x\right)\right) + \sigma^2 - x^{(1)} \tag{84}$$

is strictly increasing for fixed α (in which case $x^{(1)}$ is also fixed).

The proof of property (c) is straightforward from the definition of the function $g(\cdot)$. The proof of property (d) is given in Appendix C. □

C Proof of Lemma 2, (d)

The proof is split in a number of propositions.

Proposition 1. *For any* $\sigma^2 \leq 0.005$ *there exists* $\epsilon > 0$ *such for any* $\alpha \in (0, \hat{\alpha}]$ *and* $0 < \delta < \epsilon$ *function*

$$\eta_1(x, \alpha, \delta) \overset{def}{=} g_m\left(\frac{1}{\alpha(x+\delta)}\right) - g_m\left(\frac{1}{\alpha x}\right) \tag{85}$$

satisfies

$$\eta_1(x, \alpha, \delta) > \eta_1(\Delta, \alpha, \delta) \tag{86}$$

for any $\Delta \in [\sigma^2, 2\sigma^2]$ *and* $x \in \left(\Delta, 1 + 2\sigma^2\right]$.

Proof. The derivative of the function $\eta_1(x, \alpha, \delta)$ with respect to δ taken at $\delta = 0$ equals

$$\left.\frac{\partial \eta_1(x, \alpha, \delta)}{\partial \delta}\right|_{\delta=0} = -g'_{\mathrm{m}}\left(\frac{1}{\alpha x}\right)\frac{1}{\alpha x^2} = -g'_{\mathrm{m}}\left(y\right) y^2 \alpha \ , \tag{87}$$

where $y = 1/(\alpha x)$. Function

$$v(y) \overset{\text{def}}{=} -g'_{\mathrm{m}}\left(y\right) y^2 \tag{88}$$

is plotted in Figure 7. Function $v(y)$ is non-negative, has a single extremum, which is a maximum, at the point $y_{\mathrm{m}} \approx 3.12$, and satisfies

$$v(0) = \lim_{y \to \infty} v(y) = 0 \ .$$

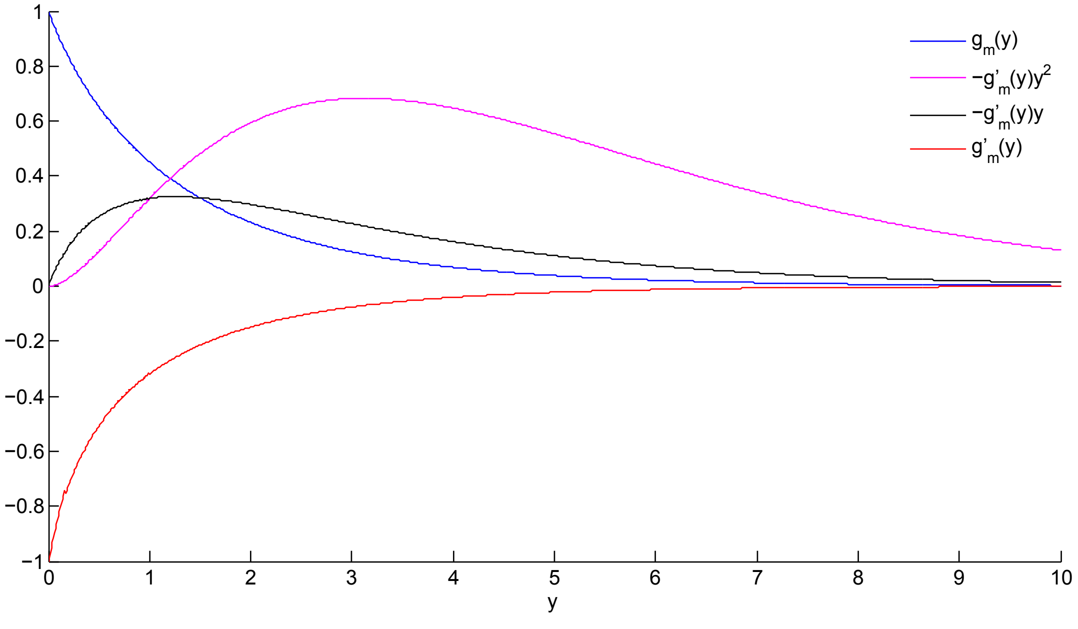

Figure 7: Plot of function $g_{\mathrm{m}}(y)$ (blue curve), $-g'_{\mathrm{m}}(y)y^2$ (magenta curve), $g'_{\mathrm{m}}(y)$ (red curve), and $-g'_{\mathrm{m}}(y)y$ (black curve).

First we show that for any $\alpha \in (0, \hat{\alpha}]$

$$v(y) > v\left(\frac{1}{\alpha\Delta}\right) \ , \qquad y \in \left[\frac{1.02}{\alpha}, \frac{1}{\alpha\Delta}\right) \ . \tag{89}$$

We consider the following two cases.

1. *Case* $\alpha < 1.02/y_m \approx 0.327$.

   Statement (89) holds since $v(y)$ is decreasing for $y > y_{\mathrm{m}}$.

2. *Case* $\alpha \geq 1.02/y_m \approx 0.327$.

We note that $-g'_{\mathrm{m}}(y) \in [0.06, 1]$ for $y \in [0, y_{\mathrm{m}}]$. Function $g'_{\mathrm{m}}(y)$ is plotted in Figure 7 (red curve). Therefore

$$v(y) \geq 0.06 y^2 \quad y \in [0, y_{\mathrm{m}}]$$

which implies

$$\min_{\alpha \in [\frac{1.02}{y_{\mathrm{m}}}, \hat{\alpha}]} \min_{y \in \left[\frac{1.02}{\alpha}, y_{\mathrm{m}}\right]} v(y) \geq 0.06 \frac{1}{\hat{\alpha}^2} = \frac{0.06}{(0.5 \log_2(1 + \frac{1}{\sigma^2}))^2} \tag{90}$$

To bound $v(y)$ for large y we use an expression for $g'_{\mathrm{m}}(y)$ derived in [19].

$$\begin{aligned} v(y) &= y \frac{e^{-y/2}}{\sqrt{2\pi}} \left[(1+y)\pi - \frac{\pi^3}{8} + \frac{\pi^3(5\pi^2 - 48)}{128 y} + \frac{241 z}{y^2} \right], \quad |z| < 1 & (91) \\ &\leq 2y^2 e^{-y/2}, & (92) \end{aligned}$$

where the last inequality is valid for $y > 5$. Since $v(y)$ is decreasing for $y \in \left[y_{\mathrm{m}}, \frac{1}{\alpha\Delta}\right]$

$$\min_{y \in \left[y_{\mathrm{m}}, \frac{1}{\alpha\Delta}\right]} v(y) = v\left(\frac{1}{\alpha\Delta}\right) \leq v\left(\frac{1}{\hat{\alpha} 2\sigma^2}\right) = v\left(\frac{1}{2\sigma^2 \log_2(1 + \frac{1}{\sigma^2})}\right) . \tag{93}$$

for any $\alpha \geq 1.02/y_{\mathrm{m}}$. It follows from (93) and (92) that

$$v\left(\frac{1}{\alpha\Delta}\right) \leq \frac{1}{2\sigma^4 \log_2^2(1 + \frac{1}{\sigma^2})} \exp\left(-\frac{1}{4\sigma^2 \log_2(1 + \frac{1}{\sigma^2})}\right) . \tag{94}$$

Finally we observe that for $\sigma^2 \leq 0.005$ the right hand side of (90) is greater than the left hand side of (94). Thus $v(y)$ attains its minimum at the point $\frac{1}{\alpha\Delta}$. This proves (89).

Using Taylor series expansion for $\eta_1(x, \alpha, \delta)$ we obtain

$$\begin{aligned} \eta_1(x, \alpha, \delta) &= \delta \left. \frac{\partial \eta_1(x, \alpha, \delta)}{\partial \delta} \right|_{\delta = 0} + \frac{1}{2}\delta^2 \left. \frac{\partial^2 \eta_1(x, \alpha, \delta)}{\partial \delta^2} \right|_{\bar{\delta}} & (95) \\ &= \delta\alpha \left(v\left(\frac{1}{\alpha x}\right) + \frac{\delta}{2} v'\left(\frac{1}{\alpha(x + \bar{\delta})}\right)\right) & (96) \end{aligned}$$

where $0 \leq \bar{\delta} \leq \delta$. Since

$$|v'(y)| \leq 0.5 \quad y \in [0, \infty) \tag{97}$$

then for sufficiently small δ (independent of α) (96) together with (89) implies (99). □

Proposition 2. *For any* $\sigma^2 \leq 0.005$ *there exists an* $\epsilon > 0$ *such for any* α *such that* $\hat{\alpha} \geq \alpha + \epsilon > \alpha > 0$ *and* $0 < \delta < \epsilon$ *function*

$$\eta_2(x, \alpha, \delta) \overset{def}{=} g_m\left(\frac{1}{(\alpha + \delta)x}\right) - g_m\left(\frac{1}{\alpha x}\right) \tag{98}$$

satisfies

$$\eta_2(x, \alpha, \delta) > \eta_2(\Delta, \alpha, \delta) \tag{99}$$

for any $\Delta \in [\sigma^2, 2\sigma^2]$ *and* $x \in \big(\Delta, 1 + 2\sigma^2\big]$.

Proof. The proof follows the lines of the proof of Proposition 1. It focuses on an analysis of a function $v_2(y) = -g'_{\mathrm{m}}(y)y$ (plotted in Figure 7, black curve) which is a scaled derivative of $\eta_2(x, \alpha, \delta)$. □

Proposition 3. *There exists an* $\epsilon > 0$ *which only depends on* σ^2 *such for any* $0 < \delta < \epsilon$ *function*

$$\phi(y, \alpha, \delta) \overset{def}{=} g_m\left(\frac{1}{(\alpha+\delta)(y + x^{(1)}(\alpha+\delta, \sigma^2))}\right) - g_m\left(\frac{1}{\alpha(y + x^{(1)}(\alpha, \sigma^2))}\right) - x^{(1)}(\alpha+\delta, \sigma^2) + x^{(1)}(\alpha, \sigma^2) > 0 \tag{100}$$

for $y \in (0, 1 + \sigma^2 - x^{(1)}(\alpha, \sigma^2)]$ *and* $\hat{\alpha} \geq \alpha + \delta > \alpha > 0$.

Proof. Lemma 1 (a) implies

$$2\sigma^2 > x^{(1)}(\alpha+\delta, \sigma^2) > x^{(1)}(\alpha, \sigma^2) > \sigma^2 \ .$$

for $\sigma^2 < 1$. For any given δ we define

$$\delta_2 \overset{\text{def}}{=} x^{(1)}(\alpha+\delta, \sigma^2) - x^{(1)}(\alpha, \sigma^2)$$

and select a sufficiently small $\epsilon > 0$ such that the conditions of Proposition 1 and Proposition 2 are satisfied simultaneously. We notice that

$$\begin{aligned}
\phi(y, \alpha, \delta) &= g_{\mathrm{m}}\left(\frac{1}{(\alpha+\delta)(y + x^{(1)}(\alpha, \sigma^2) + \delta_2)}\right) - g_{\mathrm{m}}\left(\frac{1}{(\alpha+\delta)(y + x^{(1)}(\alpha, \sigma^2))}\right) \\
&\quad + g_{\mathrm{m}}\left(\frac{1}{(\alpha+\delta)(y + x^{(1)}(\alpha, \sigma^2))}\right) - g_{\mathrm{m}}\left(\frac{1}{\alpha(y + x^{(1)}(\alpha, \sigma^2))}\right) \\
&\quad - x^{(1)}(\alpha+\delta, \sigma^2) + x^{(1)}(\alpha, \sigma^2) && (101) \\
&= \eta_1\left(y + x^{(1)}(\alpha, \sigma^2), \alpha+\delta, \delta_2\right) + \eta_2\left(y + x^{(1)}(\alpha, \sigma^2), \alpha, \delta\right) \\
&\quad - x^{(1)}(\alpha+\delta, \sigma^2) + x^{(1)}(\alpha, \sigma^2) \ . && (102)
\end{aligned}$$

Proposition 1 and Proposition 2 imply

$$\begin{aligned}
\phi(y, \alpha, \delta) &> \phi(0, \alpha, \delta) && (103) \\
&= g_{\mathrm{m}}\left(\frac{1}{(\alpha+\delta)(y + x^{(1)}(\alpha+\delta, \sigma^2))}\right) - g_{\mathrm{m}}\left(\frac{1}{\alpha(y + x^{(1)}(\alpha, \sigma^2))}\right) \\
&\quad - x^{(1)}(\alpha+\delta, \sigma^2) + x^{(1)}(\alpha, \sigma^2) && (104) \\
&= 0 && (105)
\end{aligned}$$

which finally leads to (100). □

Proposition 3 implies that $f(g(x), \alpha+\delta)$ is an increasing function of δ for any α such that $\hat{\alpha} \geq \alpha + \delta > \alpha > 0$ and $0 < \delta \leq \epsilon(\sigma^2)$. Thus, $f(g(x), \alpha+\delta)$ is an increasing function for $\alpha \in [0, \hat{\alpha}]$. Statement (d) of Lemma 2 is proved.